



Original research



Nanofluid cooling of 18650 lithium-ion batteries through wavy channel tube

Nufus Kanania^a, Muhammad Ilham Fatwa^b, Yusvardi Yusuf^b, Mekro Permana Pinem^{b,*}, Hadi Wahyudi^b, Dhimas Satria^b, Dwinanto Sukamto^b, Yustinus Purwamargapatala^c^aDepartment of Chemical Engineering, Universitas Sultan Ageng Tirtayasa, Jl. Jend. Sudirman KM3, Cielgon 42435, Banten, Indonesia^bDepartment of Mechanical Engineering, Universitas Sultan Ageng Tirtayasa, Jl. Jend. Sudirman KM3, Cielgon 42435, Banten, Indonesia^cNational Research and Innovation Agency, Serpong, Indonesia

ARTICLE INFO

Article history:

Received 31 August 2024

Received in revised form 8 December 2024

Accepted 8 December 2024

Published online 12 December 2024

Keywords:

EV industries

Battery module cooling

Cooling fluid

Thermal management

Wavy channel tube

Editor:

Bobby Kurniawan

Publisher's note:

The publisher remains neutral concerning jurisdictional claims in published maps and institutional affiliations.

ABSTRACT

The electric vehicle (EV) industries have grown; in 2023 EV sales increased by more than 30% compared to 2022. The central issue of this industry is the battery because of the cost and environmental problems. This makes efficient battery operation and condition imperative. The electric vehicle lithium-ion batteries are highly temperature-dependent for optimal performance and longevity. A cooling system is needed to maintain the temperature of the lithium-ion battery within the optimal temperature range. This study proposes nanofluid cooling based on Cellulose Nanocrystals (CNC) inside the wavy channel tube. Other fluid cooling, such as air and water, are compared. Three-dimensional (3D) transient simulation is performed by varying the cooling fluid and mass flow rate. On the other hand, experiments were conducted to validate the simulation's conformity to the battery module's temperature. The performance of the cooling fluid inside the wavy channel effectively keeps the battery heat dissipation and temperature uniformity. The nanofluid can maintain the temperature of the battery module at its optimal temperature (below 40°C), even with the lowest flow rate (5×10^{-4} kg/s).

1. Introduction

The electric vehicle (EV) industries have grown; in 2023, EV sales increased by more than 30% compared to 2022 [1]. The central issue of this industry is the battery because of the cost and environmental problems. Battery performance plays a major role in the development of electric vehicles. Lithium-ion (Li-ion) batteries are considered to be promising candidates for electric vehicles due to their advantages, such as higher energy density, lower self-discharge rate (reduced capacity without load), longer service life, and greater efficiency compared to other batteries [2]. Lithium-ion batteries generate heat due to electrochemical processes and polarization [3]. Over time, the heat generated will accumulate, causing the battery temperature to increase. Proper temperature management of an electric vehicle's lithium-ion battery is essential to maintain optimal performance, long service life, and safe battery use [4].

Lithium-ion batteries may cause slower electrochemical reactions at low temperatures, reducing

battery performance. Meanwhile, excessive temperatures can accelerate electrochemical reactions that trigger accelerated degradation of electrodes and electrolytes, thus shortening battery life, and even at too high temperatures can trigger fires and explosions [5]. This increasing temperature is more severe if many battery cells are connected in a series and parallel combination. Long-term non-uniform temperature distribution will degrade battery performance and cause state of charge (SOC) mismatches [6]. Therefore, the maximum temperature and temperature difference are important parameters that can determine the performance of the entire battery system. Under operating conditions, lithium-ion batteries can operate efficiently at the recommended temperature range of 25 °C to 40 °C, with the battery temperature difference not exceeding 5 °C [7].

It is necessary to maintain an EV battery working at optimal temperature conditions. To control the temperature in the battery system, an additional system, referred to as a battery thermal management system (BTMS), is needed. Generally, cooling systems

*Corresponding author:

Email: mekro_pinem@untirta.ac.id<http://dx.doi.org/10.62870/jiss.v10i2.28519>

consist of forced air convection, liquid cooling, phase change material (PCM), nanofluid, and combinations. Padalkar et al. [8] modified the spacing between cylindrical battery cells to improve the air-cooling efficiency of the battery pack. The results showed that the cooling performance of the battery pack was enhanced, and the battery temperature was successfully reduced without requiring additional energy or an increase in the volume size of the battery pack. The results showed that the cooling capability of the battery pack was improved, whereby the battery temperature was successfully reduced without requiring additional energy or an increase in the volume size of the battery pack.

In addition, Tang et al. [6] investigated the variation of contact angle and mass flow rate by performing numerical simulations and experiments on battery modules using multichannel wavy tube liquid cooling. The results showed that increasing the contact angle and mass flow rate positively impacted the heat dissipation efficiency and temperature uniformity of the battery module. Similarly, Rao et al. [9] inserted PCMs between prismatic batteries and liquid cooling tubes, where the study found that increasing the number of tubes can decrease the maximum temperature and temperature difference of the battery.

Nanofluid cooling contains nanoparticles suspended within the liquid base of the coolant. The addition of nanoparticles into the liquid is expected to increase the thermal conductivity of the liquid [10]. The nanoparticles are usually made of metals, oxides, carbides, and carbon nanotubes, and the liquid bases are water, ethylene glycol, and oil [11]. Nanofluids have potential in many heat transfer applications, including battery system cooling.

Sarchami et al. [12] used water and alumina nanofluids to cool battery modules; the results showed that adding alumina nanofluids and increased flow velocity significantly reduced the battery modules' maximum temperature and temperature difference. Meanwhile, Hasan et al. [13] used water and four nanofluids (SiO_2 , Al_2O_3 , ZnO , and CuO) to cooling the battery module, it was found that SiO_2 nanofluid showed the best thermal cooling and sufficient flow velocity could improve heat transfer. In addition to using the previously mentioned nanoparticle materials, the potential use of plant-based materials can also be considered to develop better and environmentally friendly cooling fluids.

Samylingam et al. [14] used a nanofluid in the form of cellulose nanocrystal (CNC) suspended in a mixed liquid base of water (W) and ethylene glycol (EG) (CNC-W+EG) as a coolant for lathe machining. The results showed that the lifetime of the lathe-cutting tool was significantly increased, and wear was reduced. This work uses nanofluids as cooling fluids to see the potential of using plant-based materials to cool battery modules.

2. Material and method

2.1. Material

The wavy channel tube is proposed as the cooling fluid to cool the battery module. The battery module comprises 13 cylindrical lithium-ion battery cells 18650-type, connected in series to generate 54 V. The cooling rate of the battery module is affected by the cooling fluid type and mass flow rate, which were analyzed based on simulation results. The effect on the thermal performance of the battery module is proposed during the discharge process with a discharge rate of 4 C.

Fig. 1 illustrates the experimental battery module without the use of cooling fluid, including the lamp load used. The battery module consists of 13 series-connected battery cells, the temperature measurement was performed by facing the FLIR towards the battery module. The charging device uses the HL54802 lithium-ion battery charger, while the discharge uses a lamp load equivalent to a discharge rate of 4C. The temperature measurement used the FLIR E5-XT WiFi device (Teledyne FLIR, US - English (United States)).

2.2. Domain and meshing

The simulation model consists of 13 cylindrical lithium-ion battery cells 18650-type connected in series and wavy channel tube, as shown in Fig. 2. The nominal voltage and nominal capacity of the lithium-ion battery cells are 3.7 V and 1.26 Ah, respectively. The characteristic parameters of the battery cell and channel geometry are listed in Table 1. The wavy channel tube is attached to the battery module to act as a bond between the batteries. The outer surface of the wavy channel tube is in contact with the side surface of the cylindrical battery cell. The wavy profile of the wavy channel tube has approximately the same radius of curvature as the cylindrical battery cell surface to ensure thermal contact. The geometry was created using SOLIDWORKS mechanical design software and imported into SPACECLAIM software to identify each part of the geometry.

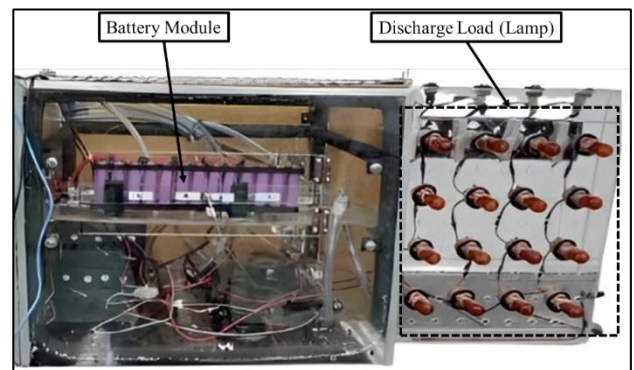


Figure 1. Experimental battery module

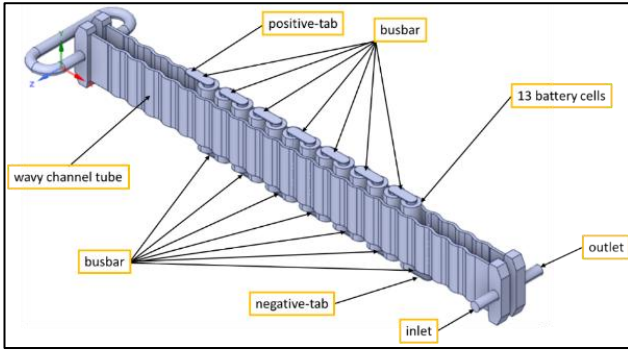


Figure 2. Battery module geometry with wavy channel tube for simulation

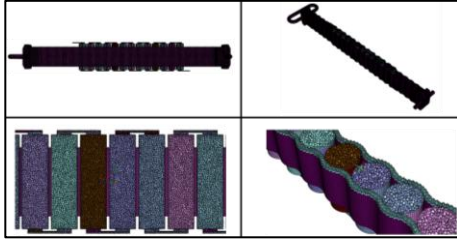


Figure 3. Polyhedral mesh of battery module with wavy channel tube for simulation

Table 1.
Parameters of battery cell and channel geometry

Parameter	Value	Parameter	Value (mm)
Capacity (Ah)	1.26	Channel Length	510
Voltage (V)	3.7	Channel Height	48
Height (mm)	65	Channel Width	2,4
Diameter (mm)	18	Inlet-Outlet Diameter	10
Mass (g)	45	Wall Thickness	0.45

Table 2.
Data for the simulation

Cooling Fluid	c_p (J/(kg · K))	k (W/(m · K))
Air	1006.43	0.242
Water	4182	0.6
W+EG	2661	0.4110
CNC-W+EG	2512.5	0.4120

Several domains are considered for the solid domain and fluid domain. The solid domain consists of the battery module, busbar, positive tab, and negative tab. Inside the battery cell are various components with different properties, making the lithium-ion battery a complex material, especially with the liquid electrolyte inside. Therefore, experimental measurements are very meaningful in determining the material properties of lithium-ion battery cells. In this study, the assumption of battery thermal properties refers to the research of Li et al. [15]. The busbar, positive tab, and negative tab are set using copper material. Table 2 shows the thermal properties of the materials used in the solid domain for simulation. Meanwhile, the fluid domain only consists of a wavy channel tube.

The tube wall is set using aluminum material. The inlet and outlet are set at both ends of the wavy channel tube. The cooling fluid flows into the wavy channel tube from the inlet, cooling the battery, and exits through the

outlet. The fluid properties are listed below [16]. The cooling fluids used include air (A), water (W), a mixture of 60% water and 40% ethylene glycol (W+EG), and 0.5% cellulose nanocrystal nanofluid suspended in a liquid base of 60% water and 40% ethylene glycol (CNC-W+EG).

Meshing is the process by which the computational domain, i.e. the control volume in the form of geometry, is divided into very small sub-volumes. The mesh for simulation was created with Ansys Fluent Meshing, where a mesh of 983069 cells with polyhedral type was used for simulation. The polyhedral mesh type was chosen because it can provide more accurate results with fewer cells [17]. The mesh for simulation is shown in Fig. 3.

The cooling system for electric vehicles is more complex, with many batteries in each module. Such systems are not evaluated in this study due to limited computational resources. The purpose of modeling in this study is to show that the modeling method can facilitate the design of the battery module and investigate the effect of the fluid to be developed as the cooling fluid of the electric vehicle battery system.

2.3. Multi-scale modeling scheme and Equivalent Circuit Model (ECM)

Modeling lithium-ion batteries is a complex challenge due to their multi-scale characteristics. The term multi-scale refers to the electrochemical reactions (anode-separator-cathode) inside the battery that are modeled into the behavior of the battery when operating, represented in the form of battery physics. The battery scale equations need to be solved to predict the temperature considering battery cooling. Therefore, a Multi-Scale-Multi-Domain (MSMD) modeling approach is required to help handle the physics in the battery domain. Eqs. (1) and (2) are differential equations solve the battery thermal and electric fields [18].

$$\nabla \cdot (\sigma_+ \nabla \varphi_+) = -(j_{ECh} - j_{short}) \quad (1)$$

$$\nabla \cdot (\sigma_- \nabla \varphi_-) = j_{ECh} - j_{short} \quad (2)$$

Where σ_+ and σ_- are the effective electrical conductivities for the positive electrode and negative electrode, φ_+ and φ_- are the phase potentials for the positive electrode and negative electrode, j_{ECh} and \dot{q}_{ECh} are the volumetric current transfer rate and heat generation due to electrochemical reactions, respectively, j_{short} and \dot{q}_{short} are the current transfer rate and heat generation rate due to internal short-circuit of the battery, respectively, and \dot{q}_{abuse} is the heat generation due to uncontrolled thermal generation. In this study, j_{short} , \dot{q}_{short} , dan \dot{q}_{abuse} are not considered because the battery module is set to operate normally.

The source terms j_{ECh} and \dot{q}_{ECh} are calculated using the electrochemical sub-model. There are several sub-models to represent battery electrochemistry. Some of the main approaches include the ECM (Equivalent Circuit Model), NTGK (Newman, Tiedemann, Gu, and

Kim), and Newman P2D (Pseudo Two Dimensional) models. In this case, the ECM approach is adopted to calculate the source term using Ansys Fluent software, specifically Ansys Fluent 2022 R2.

The ECM represents the electrochemical process inside the battery into an electrical circuit consisting of resistors and capacitors. It is based on the model proposed by Chen & Rincon [19]. The ECM model has six components consisting of V_{ocv} , R_s , and two RC parallel polarization combinations, namely R_1 , R_2 , C_1 , dan C_2 . Each component represents a different aspect of the battery. V_{ocv} is the open circuit voltage and one of the most critical parameters of a battery. R_s is the ohmic resistance, representing the internal resistance inside the battery cell, and plays a role in the voltage drop or rise when the battery works. R_1 , C_1 , R_2 , and C_2 are two parallel polarization elements, which play a role in the transient response of the battery. R_1 dan C_1 represent the speed of change in the battery, which shows the effect of the surface on the electrodes. R_1 is the resistance to flowing charge and C_1 represents the electrochemical capacitance. R_2 and C_2 represent the slower movement of the cell [18].

In simple terms, the resistor shows how easy it is for the battery to discharge current, and the capacitor is a storage of charge in the battery. For example, there is a battery with a large capacitance and a small resistance, meaning that the battery will discharge electric current faster.

This study proposes a parameter setting of the standard ECM model, where the electrical circuit parameters are modified as a function of SOC and depending on the battery cell temperature. The modification is implemented using the estimation table in Ansys Fluent. The circuit is solved using the current-voltage relationship equation. Then, the source terms are calculated and distributed in volume as shown in Eqs. (3) and (4), where Vol denotes the battery volume and I is the electric current.

$$\dot{q}_{ECh} = \frac{I}{Vol} \left[V_{ocv} - (\varphi_+ - \varphi_-) - T \frac{dU}{dT} \right] \quad (3)$$

$$j_{ECh} = \frac{I}{Vol} \quad (4)$$

In modeling the lithium-ion battery cooled by the wavy channel tube, the conjugate heat transfer problem needs to be considered. The conductive equation with the battery cell domain heat source term governing heat transfer is shown in Equation 5. Where ρ , k_{cell} , and c_p are the density, thermal conductivity, and heat capacity of the battery, respectively [15].

$$\rho c_p \frac{\partial T}{\partial t} = k_{cell} \nabla T + \dot{q}_{ECh} \quad (5)$$

2.4. Boundary conditions

Numerical simulations were performed using Ansys Fluent software, specifically Ansys Fluent 2022 R2. Three-dimensional thermal modeling for cooling the

battery module using a wavy channel tube was conducted with mass flow rates 5×10^{-4} kg/s, 10×10^{-4} kg/s, and 15×10^{-4} kg/s. The Reynolds number (Re) is considered from these mass flow rates in determining the type of flow. The Re number is defined by Eq. (6), as expressed by [20].

$$Re = \frac{\rho v D}{\mu} \quad (6)$$

where, ρ = cooling fluid density; v = cooling fluid flow velocity; D = hydraulic channel diameter (2.9 mm); and μ = cooling fluid viscosity. In this study, the laminar flow model was chosen because the Re value of each mass flow rate with each cooling fluid is less than 2300.

In modeling the cooling of the battery module, the conductive equation without heat source terms is used on the aluminum wavy channel tube. In addition, for the fluid domain, mass conservation, Navier-Stokes (N-S) equations, and convective diffusion temperature equations are applied to the cooling fluid flow. The flow is solved first for each simulation using the Coupled scheme with second-order accuracy until convergence. The Energy and Multi-Scale Multi-Domain (MSMD) models were enabled to generate electro-thermal battery. ECM is used to model the electro-thermal behavior of lithium-ion battery cells. The nominal capacity of the battery and the applied discharge rate were entered as 1.26 Ah and 4C, respectively. In addition, the minimum and maximum stop voltage values were 3 V and 4.3 V, respectively. Each lithium-ion battery cell is electrically connected with a busbar to form a 13S1P (13 series and 1 parallel) battery module circuit. The battery module has a positive tab and a negative tab connected to the load for discharge.

The identification of ECM parameters (V_{ocv} , R_s , R_1 , R_2 , C_1 , dan C_2) is done using the battery cell hppc (hybrid pulse power characterization) test approach [17]. In this hppc test, a series of discharge pulses are given to battery cells at different SOC, and the voltage and amperage are measured. The battery cells are fully charged to 100% SOC, then discharged in stages of every 10% SOC with a discharge pulse if 30 seconds, resting 10 minutes at each stage of 10% SOC [20]. This procedure was repeated with different temperature conditions, namely 25 °C, 35 °C, and 45 °C. The hppc test data was entered into the parameter estimation tool for batteries in Ansys Fluent [18], resulting in the ECM parameters of the battery being V_{ocv} , R_s , R_1 , R_2 , C_1 , and C_2 .

The inlet and outlet boundaries are set as mass flow inlet and outflow for the cooling fluid domain, respectively. Coupled heat transfer between liquid and solid regions is considered, including the contact surface between the wavy channel tube and the battery module. The battery surface is set as a natural convection boundary condition with a constant heat transfer coefficient of $5 \text{ W/m}^2\text{°C}$ and the free flow temperature is set to 30 °C, and radiation heat transfer is neglected due to small temperature variations [12].

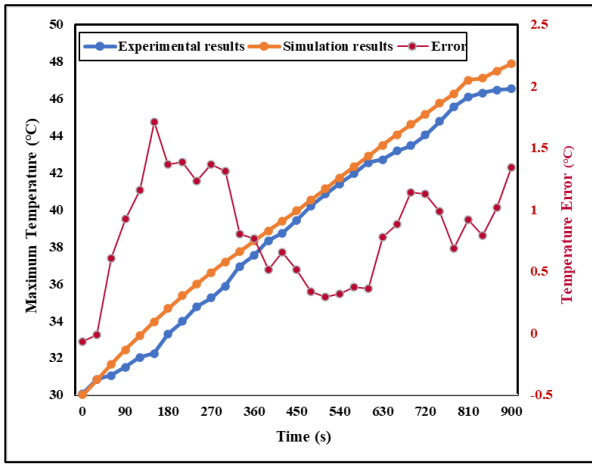


Figure 4. Comparison of battery module temperature increases between simulation and experimental results without cooling fluid under 4C discharge rate conditions

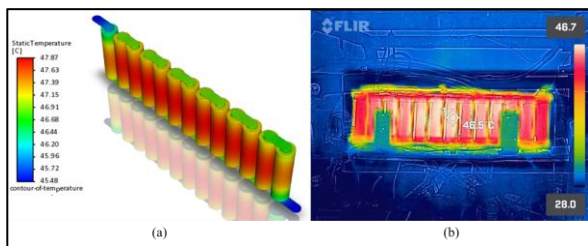


Figure 5. Temperature distribution contours of the batteries (a) simulation results and (b) experimental results without cooling fluid under the condition of 4C discharge rate

3. Results and discussions

3.1. Model validation

Model validation consists of comparing experimental data with numerical simulation model predictions. In the validation of the model, the thermal performance of the proposed battery module is measured in experimental experiments under conditions without cooling fluid. The battery tested in this experiment is a lithium-ion battery 18650-type. The experimental setup consists of the battery module, charge-discharge device, and battery module temperature measurement.

In this study, when the room temperature was 30°C, the battery module was discharged from its full state until it was discharged by turning on the light load (discharge rate 4C). The temperature data of the battery module read by the FLIR was recorded every 30 seconds until the light load turned off, which declared the battery module to be discharged, which is about 900 seconds. The experimental and simulated data under these conditions are compared in Fig. 4. The simulated temperature increase is predicted to match the experimental results without cooling fluid. The difference between the experimental and simulated data (temperature error) is also listed. The maximum temperatures of the simulated and experimental results are 47.87 °C and 46.7 °C, respectively, with an error percentage of 2.44%.

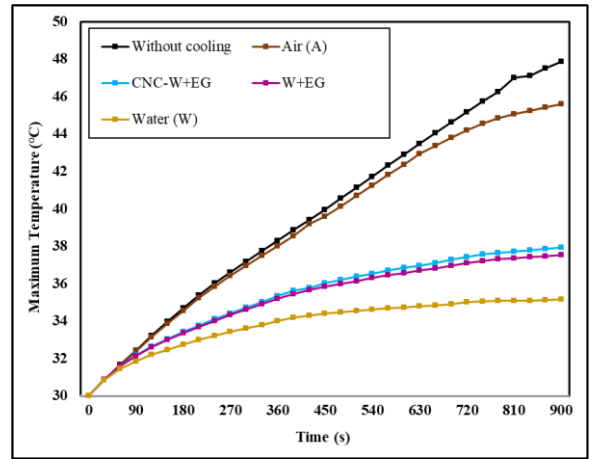


Figure 6. The maximum temperature increases of battery modules in different cooling fluids with a mass flow rate of 5×10^{-4} kg/s

Fig. 5 shows the temperature distribution contour of the battery module obtained at 900 seconds during discharge without cooling fluid. It can be observed that the battery module temperature is uniformly distributed between cells and exceeds the optimal temperature range. Surface hot spots occur at the body region between cells, with lower temperature regions at the busbar, positive tab, and negative tab. In this case, it can be assumed that the heat at the intercell body region has the highest temperature, which confirms the importance of cooling the battery module to avoid excessive temperatures and ensure safety. With these results, all simulations were carried out using a cooling fluid.

The thermal performance of the proposed battery module cooling is affected by the type of fluid used and the mass flow rate. Therefore, both variables were investigated. The temperature of the battery module was monitored at a discharge rate of 4C to investigate the cooling performance. The contact surface between the battery module and the wavy channel tube has approximately the same radius of curvature as the cylindrical battery cell surface.

3.2. Effect of the cooling fluid

The heat the battery module generates during operation is cooled by the cooling fluid flowing inside the wavy channel tube. The cooling performance is compared using four fluid types: air (A), water (W), W+EG, and CNC-W+EG nanofluid. In this case, CNC-W+EG nanofluid is particularly interesting to determine the effect of plant-based nanoparticles in cooling the battery module.

Fig. 6 shows the increasing trend of the maximum temperature of the battery module with operating time, which is cooled using different cooling fluids with a mass flow rate of 5×10^{-4} kg/s at a discharge rate of 4C. The cooling fluid flowing inside the wavy channel tube controls the heat generated by the battery module. With the cooling fluid, the maximum temperature of the battery module can be lowered to not exceed the optimal temperature range.

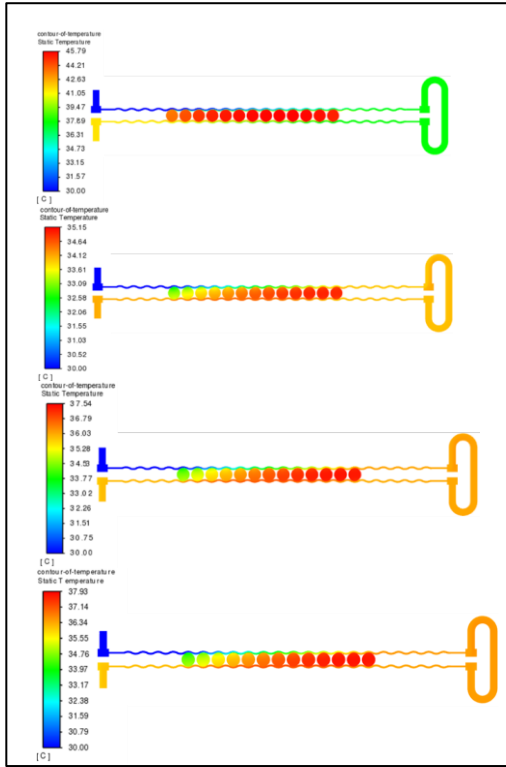


Figure 7. Maximum temperature distribution of battery modules at different cooling fluids: (a) Air; (b) Water; (c) W+EG; (d) CNC-W+EG with a mass flow rate of 5×10^{-4} kg/s

Table 3.

The maximum temperature (°C) of battery modules with different cooling fluids and mass flow rates under 4C discharge rate conditions

Cooling Fluid	Mass Flow Rate (kg/s)		
	5×10^{-4}	10×10^{-4}	15×10^{-4}
Air (A)	45.79	40.74	38.43
Water (W)	35.15	33.03	32.32
W+EG	37.54	34.40	33.32
CNC-W+EG	37.93	34.60	33.42

The simulation results show that the effect of air inside the wavy channel to cooling the battery module at the lowest flow rate has not reached the optimal temperature. However, it was found that air managed to reach the optimal temperature at a flow rate of 15×10^{-4} kg/s, and it is predicted that increasing the mass flow rate can reduce the temperature of the battery module more effectively. Unlike air, liquids as cooling fluids, namely water, W+EG, and CNC-W+EG nanofluids, can reach the optimal temperature of the battery at the lowest flow rate. Water is the fluid that can control the lowest maximum temperature of the battery module, followed by W+EG and CNC-W+EG. However, besides the good performance of liquids in cooling the battery, it also requires a more complicated construction that requires a higher cost than air as a cooling fluid [6] in implementing different cooling systems. Based on the simulation results at a flow rate of 15×10^{-4} kg/s with cooling fluids of air (A), water (W), W+EG, and CNC-W+EG nanofluids, the maximum temperatures obtained were 45.79 °C, 35.15 °C, 37.54 °C, and 37.93 °C, respectively.

The cooling fluid flow enters the wavy channel tube through the inlet at 30 °C (colored blue in Fig. 7). The cooling fluid absorbs heat from the battery module and carries the heat to the outlet for disposal, so the outlet temperature is higher than the inlet. The simulation results show that the battery with a lower temperature is found in the battery closest to the inlet, followed by the battery with increasing temperature. However, the battery that is farthest from the inlet does not have the highest temperature. This is predicted because after the fluid circulates, the fluid absorbs that battery's heat first, followed by the other batteries. In the air-cooling fluid, the maximum temperature is obtained at the 10th battery from the inlet. While in the water-cooling fluid, W+EG, and CNC-W+EG, the maximum temperature is obtained at the 12th battery from the inlet.

The cooling fluid's performance towards reducing the battery module's maximum temperature depends on the fluid's ability to absorb and carry the heat generated by the battery module. Fluids are known to have a better ability to transfer heat than air. In simulations, this is represented by fluid properties parameters, such as density, specific heat, thermal conductivity, and viscosity. These parameter properties describe the actual properties of the fluid. The most influential properties in transferring heat are thermal conductivity and specific heat.

Air has much lower thermal property values than liquids. The trend of increasing the temperature of the battery module with air cooling fluid is also observed to approach without cooling fluid until it finally moves away so that at the end of discharge, air can only reduce the maximum temperature of the battery module by 2.08 °C. On the other hand, water as a cooling fluid has superior thermal properties compared to other cooling fluids. It can be seen that water absorbs and carries heat better, reducing the maximum temperature by 12.72 °C compared to no cooling fluid. Meanwhile, W+EG and CNC-W+EG have thermal properties that are not much different. The effect can be seen with the trend of increasing the maximum temperature of the battery module in both fluids that go hand in hand; at the end of the discharge, the maximum temperature difference obtained is 0.39 °C.

The CNC-W+EG nanofluid was not predicted to be the most effective in this case, but the results showed that it could control the temperature of the battery module at its optimal temperature, even with the lowest flow rate.

3.3. Effect of flow rate

The cooling fluid flowing and circulating inside the wavy channel tube controls the accumulation of heat generated by the battery module. The fluid flow rate greatly controls the cooling efficiency of the battery module. To study the temperature distribution with flow rate under the condition of discharge rate of 4C and ambient temperature of 30 °C, the range of flow rate is set to 5×10^{-4} kg/s, 10×10^{-4} kg/s, dan 15×10^{-4} kg/s.

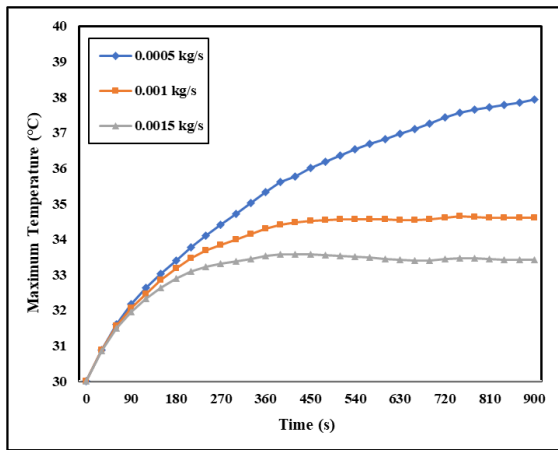


Figure 8. Effect of CNC-W+EG nanofluid cooling fluid on battery module temperature

The maximum temperature of the battery module with different cooling fluids and mass flow rates is shown in Table 3. Meanwhile, the cooling fluid shown here is CNC-W+EG nanofluid to illustrate the influence of mass flow rate. The temperature increases during the discharge process and increases steadily after reaching a certain time during operation. As shown in Fig. 8, increasing the cooling fluid flow rate from 5×10^{-4} kg/s to 15×10^{-4} kg/s decreases the maximum temperature in the battery module by about 0 – 4.51 °C.

Increasing the flow rate results in a significant decrease in the maximum temperature, as described in the increasing trend of the maximum temperature of the battery modules. In addition, it is also found that increasing the flow rate dramatically reduces the temperature difference in the battery modules. There is a low heat transfer rate at low flow rates, resulting in heat buildup in the battery, especially in batteries far from the inlet. However, the cooling fluid flowing in the wavy channel tube with a mass flow rate that is too high has a large amount of unused cooling capacity and a high pump head. An adequate battery cooling system in electric vehicles can ensure consistent performance, especially when heavy loads such as high speeds or on uphill roads require high discharge power.

4. Conclusions

High temperatures exceeding the optimal range do not immediately impact battery performance. However, high temperatures must be avoided to protect the battery components from degrading, which reduces battery performance in the long term. In this work, the effect of different cooling fluids and mass flow rates on the thermal performance of the battery module was investigated. The temperature distribution was monitored to measure the heat transfer capacity.

Different cooling fluids show different cooling effects. The Maximum temperature can be maintained not exceeding 40°C during the discharge process with a discharge rate of 4C at a low flow rate (5×10^{-4} kg/s), except that air is only able to reach the optimum temperature of the battery at a flow rate of 15×10^{-4} kg/s. The CNC-W+EG nanofluid can control the temperature

of the battery module at its optimal temperature (below 40°C), even at the lowest flow rate (5×10^{-4} kg/s). Increasing the mass flow rate of the cooling fluid can significantly reduce the battery module's maximum temperature.

Future research could be conducted on metal-based nanoparticles. Although environmental considerations should be taken seriously.

Declaration statement

Nufus Kanani: **Arrange the data collection and drafting of the manuscript.** Muhammad Ilham Fatwa: **Collecting data.** Hadi Wahyudi: **Supervised the simulation part.** Yusvardi Yusuf, Dhimas Satria, Dwinanto Sukanto, Deddy Triawan: **editing table and graph.** Yustinus Purwamargapratala: **Supervised the experimental part.** Mekro Permana Pinem: **Conceptualized original idea, developed methodology, and supervised research.**

Acknowledgement

The authors thank the Ministry of Education and Culture Indonesia, Universitas Sultan Ageng Tirtayasa, and National Research and Innovation Agency Indonesia for their invaluable support.

Disclosure statement

The authors declare no conflicts of interest in publishing this work.

Funding statement

This research was funded by the Directorate General of Higher Education, Research, and Technology under contract number 0557/E5.5/AL.04/2023.

Data availability statement

The data in this work are available from the corresponding author upon reasonable request.

References

- [1] "Trends in electric cars - Global EV Outlook 2024 - Analysis," IEA. Accessed: Aug. 26, 2024. [Online]. Available: <https://www.iea.org/reports/global-ev-outlook-2024/trends-in-electric-cars>
- [2] W. Wu, S. Wang, W. Wu, K. Chen, S. Hong, and Y. Lai, "A critical review of battery thermal performance and liquid based battery thermal management," *Energy Conversion and Management*, vol. 182, pp. 262–281, Feb. 2019, doi: [10.1016/j.enconman.2018.12.051](https://doi.org/10.1016/j.enconman.2018.12.051).
- [3] N. Adhikari, R. Bhandari, and P. Joshi, "Thermal analysis of lithium-ion battery of electric vehicle using different cooling medium," *Applied Energy*, vol. 360, p. 122781, Apr. 2024, doi: [10.1016/j.apenergy.2024.122781](https://doi.org/10.1016/j.apenergy.2024.122781).
- [4] M. Malik, I. Dincer, M. Rosen, and M. Fowler, "Experimental Investigation of a New Passive Thermal Management System for a Li-Ion Battery Pack Using

- Phase Change Composite Material,” *Electrochimica Acta*, vol. 257, pp. 345–355, Dec. 2017, doi: [10.1016/j.electacta.2017.10.051](https://doi.org/10.1016/j.electacta.2017.10.051).
- [5] S. Ma et al., “Temperature effect and thermal impact in lithium-ion batteries: A review,” *Progress in Natural Science: Materials International*, vol. 28, no. 6, pp. 653–666, Dec. 2018, doi: [10.1016/j.pnsc.2018.11.002](https://doi.org/10.1016/j.pnsc.2018.11.002).
- [6] Z. Tang, X. Min, A. Song, and J. Cheng, “Thermal Management of a Cylindrical Lithium-Ion Battery Module Using a Multichannel Wavy Tube,” *Journal of Energy Engineering*, vol. 145, no. 1, p. 04018072, Feb. 2019, doi: [10.1061/\(ASCE\)EY.1943-7897.0000592](https://doi.org/10.1061/(ASCE)EY.1943-7897.0000592).
- [7] R. D. Widyantara, S. Zulaihah, F. B. Juangsa, B. A. Budiman, and M. Aziz, “Review on Battery Packing Design Strategies for Superior Thermal Management in Electric Vehicles,” *Batteries*, vol. 8, no. 12, Art. no. 12, Dec. 2022, doi: [10.3390/batteries8120287](https://doi.org/10.3390/batteries8120287).
- [8] A. B. Padalkar, M. B. Chaudhari, and A. M. Funde, “Computational investigation for reduction in auxiliary energy consumption with different cell spacing in battery pack,” *Journal of Energy Storage*, vol. 65, p. 107265, Aug. 2023, doi: [10.1016/j.est.2023.107265](https://doi.org/10.1016/j.est.2023.107265).
- [9] Z. Rao, Q. Wang, and C. Huang, “Investigation of the thermal performance of phase change material/mini-channel coupled battery thermal management system,” *Applied Energy*, vol. 164, pp. 659–669, Feb. 2016, doi: [10.1016/j.apenergy.2015.12.021](https://doi.org/10.1016/j.apenergy.2015.12.021).
- [10] M. A. Abdelkareem et al., “Battery thermal management systems based on nanofluids for electric vehicles,” *Journal of Energy Storage*, vol. 50, p. 104385, Jun. 2022, doi: [10.1016/j.est.2022.104385](https://doi.org/10.1016/j.est.2022.104385).
- [11] S. Kakaç, H. Liu, and A. Pramuanjaroenkij, *Heat Exchangers: Selection, Rating, and Thermal Design, Third Edition*, 3rd ed. Boca Raton: CRC Press, 2012. doi: [10.1201/b11784](https://doi.org/10.1201/b11784).
- [12] A. Sarchami et al., “A novel nanofluid cooling system for modular lithium-ion battery thermal management based on wavy/stair channels,” *International Journal of Thermal Sciences*, vol. 182, p. 107823, Dec. 2022, doi: [10.1016/j.ijthermalsci.2022.107823](https://doi.org/10.1016/j.ijthermalsci.2022.107823).
- [13] H. A. Hasan et al., “Numerical investigation on cooling cylindrical lithium-ion-battery by using different types of nanofluids in an innovative cooling system,” *Case Studies in Thermal Engineering*, vol. 49, p. 103097, Sep. 2023, doi: [10.1016/j.csite.2023.103097](https://doi.org/10.1016/j.csite.2023.103097).
- [14] L. Samylingam et al., “Thermal analysis of cellulose nanocrystal-ethylene glycol nanofluid coolant,” *International Journal of Heat and Mass Transfer*, vol. 127, pp. 173–181, Dec. 2018, doi: [10.1016/j.ijheatmasstransfer.2018.07.080](https://doi.org/10.1016/j.ijheatmasstransfer.2018.07.080).
- [15] Y. Li, Z. Zhou, and W.-T. Wu, “Three-dimensional thermal modeling of Li-ion battery cell and 50 V Li-ion battery pack cooled by mini-channel cold plate,” *Applied Thermal Engineering*, vol. 147, pp. 829–840, Jan. 2019, doi: [10.1016/j.applthermaleng.2018.11.009](https://doi.org/10.1016/j.applthermaleng.2018.11.009).
- [16] K. Farhana et al., “Experimental Studies on Thermo-Physical Properties of Nanocellulose–Aqueous Ethylene Glycol Nanofluids,” *Journal of Advanced Research in Materials Science*, vol. 69, pp. 1–15, Jun. 2020, doi: [10.37934/arms.69.1.115](https://doi.org/10.37934/arms.69.1.115).
- [17] M. Sosnowski, J. Krzywanski, K. Grabowska, and R. Gnatowska, “Polyhedral meshing in numerical analysis of conjugate heat transfer,” *EPJ Web Conf.*, vol. 180, p. 02096, 2018, doi: [10.1051/epjconf/201818002096](https://doi.org/10.1051/epjconf/201818002096).
- [18] “Add on modules in Fluent,” Ansys Learning Forum | Ansys Innovation Space. Accessed: Aug. 27, 2024. [Online]. Available: <https://innovationspace.ansys.com/forum/forums/topic/add-on-modules-in-fluent/>
- [19] M. Chen and G. A. Rincon-Mora, “Accurate electrical battery model capable of predicting runtime and I-V performance,” *IEEE Transactions on Energy Conversion*, vol. 21, no. 2, pp. 504–511, Jun. 2006, doi: [10.1109/TEC.2006.874229](https://doi.org/10.1109/TEC.2006.874229).
- [20] J. Cimbala, *Fluid Mechanics: Fundamentals and Applications*, 4th Edition. Mc Graw Hill, 2017.